

1 **Change in turbopause altitude at 52° and 70°N**

2

3 C. M. Hall¹, S. E. Holmen^{1,2,5}, C. E. Meek³, A. H. Manson³ and S. Nozawa⁴

4 ¹ Tromsø Geophysical Observatory, UiT - The Arctic University of Norway, Tromsø,
5 Norway

6 ² The University Centre in Svalbard, Norway

7 ³ University of Saskatchewan, Saskatoon, Canada

8 ⁴ Nagoya University, Nagoya, Japan

9 ⁵ Birkeland Centre for Space Science, Bergen Norway

10

11 Correspondence to:

12 C. M. Hall (chris.hall@tgo.uit.no)

13

14 Full institute address

15 UiT - The Arctic University of Norway,

16 Tromsø Geophysical Observatory,

17 9037 Tromsø,

18 Norway

19 **Abstract**

20 The turbopause is the demarcation between atmospheric mixing by turbulence (below) and
21 molecular diffusion (above). When studying concentrations of trace species in the
22 atmosphere, and particularly long-term change, it may be important to understand processes
23 present, together with their temporal evolution that may be responsible for redistribution of
24 atmospheric constituents. The general region of transition between turbulent and molecular
25 mixing coincides with the base of the ionosphere, the lower region in which molecular
26 oxygen is dissociated, and, at high latitude in summer, the coldest part of the whole
27 atmosphere.

28 This study updates previous reports of turbopause altitude, extending the time series by half a
29 decade, and thus shedding new light on the nature of change over solar-cycle timescales.

30 Assuming there is no trend in temperature, at 70°N there is evidence for a summer trend of
31 ~1.6 km/decade, but for winter and at 52°N there is no significant evidence for change at all.

32 If the temperature at 90 km is estimated using meteor trail data, it is possible to estimate a
33 cooling rate, which, if applied to the turbopause altitude estimation, fails to alter the trend
34 significantly irrespective of season.

35 The observed increase in turbopause height supports a hypothesis of corresponding negative
36 trends in atomic oxygen density, [O]. This supports independent studies of atomic oxygen
37 density, [O], using mid-latitude timeseries dating from 1975, which show negative trends
38 since 2002..

39

40 **Introduction**

41 The upper mesosphere and lower thermosphere (UMLT) regime of the atmosphere exhibits a
42 number of features, the underlying physics of which are interlinked and, relative to processes
43 at other altitudes, little understood. At high latitude, the summer mesopause, around 85km is
44 the coldest region in the entire atmosphere. The UMLT is, inter alia, characterized by the
45 base of the ionosphere, dissociation of molecular species (for example oxygen) by sunlight,
46 and, the focus in this study, the transition from turbulent mixing to distribution of constituents
47 by molecular diffusion. The altitude at which transition turbulence-dominated mixing gives
48 way to molecular diffusion is known as the turbopause, and typically occurs around 100 km,
49 but displaying a seasonal variation, being lower in summer (e.g. ~95 km) and higher in winter
50 (e.g. ~110km) (Danilov et al., 1979). Many processes in the UMLT are superimposed and
51 linked. One example is where the mesopause temperature structure determines the altitude
52 dependence of breaking of upwardly propagating gravity waves (e.g. McIntyre, 1991) and
53 thus generation of turbulence. Indeed, the concept of a “wave turbopause” was proposed by
54 Offermann et al. (2007) and compared with the method used forthwith by Hall et al. (2008).
55 Prevailing winds filter or even inhibit propagation of gravity waves generated in the lower
56 atmosphere and the static stability (or lack of it) of the atmosphere dictates the vertical
57 distribution of gravity wave saturation and breaking. The generation of turbulence and its
58 height distribution vary with season and similarly affect the turbopause altitude (e.g. Hall et
59 al., 1997). Turbulence is somewhat distributed through the high latitude winter mesosphere,
60 whereas in summer the gravity waves "save their energy" more until reaching the "steep
61 beach" (a visualization attributable to M. E. McIntyre - private communication) of the
62 summer mesopause near 85km. Vertical transport by turbulent mixing and horizontal
63 transport by winds redistribute constituents such as atomic oxygen, hydroxyl and ozone.

64 Thus, long-term change in trace constituents cannot be fully explained in isolation from
65 studies of corresponding change in temperature and neutral dynamics.

66 One means of locating the turbopause is to measure the concentration of particular species as
67 a function of height and noting where the constituents exhibit scale heights that depend on
68 their respective molecular weights, e.g. Danilov et al., (1979). Detection of turbulence and
69 estimation of its intensity is non-trivial because direct measurement by radar depends on
70 turbulent structures being “visible” due to small discontinuities in refractive index, e.g.
71 Schlegel et al. (1978) and Briggs (1980). At 100km, this implies some degree of ionisation
72 and even in situ detectors often depend on ionisation as a tracer (e.g. Thrane et al. 1987). A
73 common means of quantifying turbulent intensity is the estimation of turbulent energy
74 dissipation rate, ε . In the classical visualization of turbulence in two dimensions, large
75 vortices generated by, for example breaking gravity waves or wind shears form progressively
76 smaller vortices (eddies) until inertia is insufficient to overcome viscous drag in the fluid.
77 Viscosity then "removes" kinetic energy and transforms it to heat. This "cascade" from large-
78 scale vortices to the smallest scale eddies capable of being supported by the fluid, and
79 subsequent dissipation of energy, was proposed by Kolmogorov (1941) but more accessibly
80 described by Batchelor (1953) and (e.g.) Kundu (1990). At the same time, a minimum rate of
81 energy dissipation by viscosity is supported by the atmosphere (defined subsequently). The
82 altitude at which these two energy dissipation rates are equal is also a definition of the
83 turbopause and corresponds to the condition where the Reynolds number, the ratio between
84 inertial and viscous forces, is unity.

85 The early work to estimate turbulent energy dissipation rates using medium frequency (MF)
86 radar by Schlegel et al. (1978) and Briggs (1980) was adopted by Hall et al. (1998a). The
87 reader is referred to these earlier publications for a full explanation, but in essence, velocity
88 fluctuations relative to the background wind give rise to fading with time of echoes from

89 structures in electron density drifting through the radar beam. While the drift is determined
90 by cross-correlation of signals from spaced receiver antennas, autocorrelation yields fading
91 times which may be interpreted as velocity fluctuations (the derivation of which is given in
92 the following section). The squares of the velocity perturbations can be equated to turbulent
93 kinetic energy and then, when divided by a characteristic timescale become energy
94 dissipation rates. Energy is conserved in the cascade to progressively smaller and more
95 numerous eddies such that the energy dissipation rate is representative of the ultimate
96 conversion of kinetic energy to heat by viscosity. Hall et al. (1998b and 2008) subsequently
97 applied the turbulent intensity estimation to identification of the turbopause. The latter study,
98 which offers a detailed explanation of the analysis, compares methods and definitions and
99 represents the starting point for this study. In addition, Hocking (1983 and 1996) and
100 Vandeppeer and Hocking (1993) offer a critique on assumptions and pitfalls pertaining to
101 observation of turbulence using radars. For the radars to obtain echoes from the UMLT, a
102 certain degree of ionization must be present and daylight conditions yield better results than
103 night-time, and similarly results are affected by solar cycle variation. However, there is a
104 trade-off: too little ionization prevents good echoes while too much gives rise to the problem
105 of group delay of the radar wave in the ionospheric D-region. Space weather effects that are
106 capable of creating significant ionization in the upper mesosphere are infrequent, and aurora
107 normally occur on occasional evenings at high latitude, and then only for a few hours
108 duration at the most. Of the substantial dataset used in this study, however, only a small
109 percentage of echo profiles are expected to be affected by auroral precipitation that would
110 cause problematic degrees of ionisation below the turbopause. While it must be accepted that
111 group delay at the radar frequencies used for the observations reported here cannot be
112 dismissed, the MF-radar method is the only one that has been available for virtually
113 uninterrupted measurement of turbulence in the UMLT region over the past decades.

114 Full descriptions of the radar systems providing the underlying data used here are to be found
 115 in Hall (2001) and Manson and Meek (1991) and the salient features of the radars, relevant
 116 for this study are given in Table 1.

117

118 **Analysis methodology**

119 The characteristic fading time of the signal, τ_c , is used to define an indication of the upper
 120 limit for turbulent energy dissipation present in the atmosphere, ε' , as explained above. First,
 121 velocity fluctuations, v' relative to the background wind are identified as:

$$122 \quad v' = \frac{\lambda \sqrt{\ln 2}}{4\pi \tau_c} \quad (1)$$

123 where λ is the radar wavelength. This relationship has been presented and discussed by
 124 Briggs (1980) and Vandeppeer and Hocking (1993). In turn v'^2 can be considered to represent
 125 the turbulent kinetic energy of the air such that the rate of dissipation of this energy is
 126 obtained by dividing by a characteristic timescale. If the Brunt-Väisälä period T_B ($= 2\pi/\omega_B$
 127 where ω_B is the Brunt-Väisälä frequency in rad s^{-1}) can be a characteristic timescale, then it
 128 has been proposed that:

$$129 \quad \varepsilon' = 0.8v'^2/T_B \quad (2)$$

130 the factor 0.8 being related to an assumption of a total velocity fluctuation (see Weinstock,
 131 1978). Alternatively, this can be expressed as:

$$132 \quad \varepsilon' = 0.8v'^2\omega_B/2\pi \quad (3)$$

133 wherein the Brunt-Väisälä frequency is given by

$$134 \quad \omega_B = \sqrt{\left(\frac{dT}{dz} + \frac{g}{c_p}\right)\frac{g}{T}} \quad (4)$$

135 where T is the neutral temperature, z is altitude, g is the acceleration due to gravity and c_p is
 136 the specific heat of the air at constant pressure. Due to viscosity, there is a minimum energy
 137 dissipation rate, ε_{\min} , present in the atmosphere, given by

$$138 \quad \varepsilon_{\min} = \omega_B^2 \nu / \beta \quad (5)$$

139 where ν is the kinematic viscosity. The factor β , known as the mixing or flux coefficient
 140 (Oakey, 1982; Fukao et al., 1994; Pardyjac et al., 2002), is related to the flux Richardson
 141 Number R_f ($\beta = R_f / (1 - R_f)$). R_f is in turn related to the commonly used gradient Richardson
 142 number, Ri by the ratio of the momentum to thermal turbulent diffusivities, or turbulent
 143 Prandtl number (e.g. Kundu 1990). Fukao et al. (1994) proposed 0.3 as a value for β . The
 144 relationships are fully described by Hall et al. (2008). To use the MF radar system employed
 145 here to estimate turbulence is not well suited to estimating Ri due to the height resolution of
 146 3km; moreover more detailed temperature information would be required to arrive at R_f .

147 Anywhere in the atmosphere, energy dissipation is by the sum of the available processes. In
 148 this study, therefore, the turbulent energy dissipation rate can be considered the total rate
 149 minus that corresponding to viscosity:

$$150 \quad \varepsilon = \varepsilon' - \varepsilon_{\min} \quad (6)$$

151 Importantly, the kinematic viscosity is given by the dynamic viscosity, μ , divided by the
 152 density, ρ :

$$153 \quad \nu = \mu / \rho \quad (7)$$

154 Thus, since density is inversely proportional to temperature, kinematic viscosity is
 155 (approximately) linearly dependent on temperature; ω_B^2 is inversely proportional to
 156 temperature and therefore ε_{\min} is approximately independent of temperature. On the other
 157 hand, ε' is proportional to ω_B and therefore inversely proportional to the square root of
 158 temperature.

159 If we are able to estimate the energy dissipation rates described above, then the turbopause
 160 may be identified as the altitude at which $\varepsilon = \varepsilon_{\min}$. This corresponds to equality of inertial and
 161 viscous effects and hence the condition where Reynolds number, Re , is unity as explained
 162 earlier.

163 To implement the above methodology, temperature data are required. Since observational
 164 temperature profiles cannot be obtained reliably, NRLMSISE-00 empirical model (Picone et
 165 al., 2002) profiles are, of necessity, used in the derivation of turbulent intensity from MF-
 166 radar data. The reasons for this are discussed in detail in the following section. While a
 167 temperature profile covering the UMLT region is not readily available by ground-based
 168 observations from Tromsø, meteor-trail echo fading times measured by the Nippon/Norway
 169 Tromsø Meteor Radar (NTMR) can be used to yield neutral temperatures at 90 km altitude.
 170 Any trend in temperature can usefully be obtained (the absolute values of the temperatures
 171 being superfluous since they are only available for one height). The method is exactly the
 172 same as used by Hall et al. (2012) to determine 90 km temperatures over Svalbard (78°N)
 173 using a radar identical to NTMR. Hall et al. (2005) investigate the unsuitability of meteor
 174 radar data for temperature determination above ~95km and below ~85 km. In summary:
 175 ionization trails from meteors are observed using a radar operating at a frequency less than
 176 the plasma frequency of the electron density in the trail (this is the so-called "underdense"
 177 condition). It is then possible to derive ambipolar diffusion coefficients D from the radar echo
 178 decay times, τ_{meteor} (as distinct from the corresponding fading time for the medium-frequency
 179 radars) according to:

$$180 \quad \tau_{meteor} = \frac{\lambda^2}{16\pi^2 D} \quad (8)$$

181 wherein λ is the radar wavelength. Thereafter the temperature T may be derived using the
 182 relation:

$$183 \quad T = \sqrt{\frac{P \cdot D}{6.39 \times 10^{-2} K_0}} \quad (9)$$

184 where P is the neutral pressure and K_0 is the zero field mobility of the ions in the trail (here
 185 we assume $K_0 = 2.4 \times 10^{-4} \text{ m}^{-2} \text{ s}^{-1} \text{ V}^{-1}$) (McKinley, 1961; Chilson et al., 1996; Cervera and
 186 Reid, 2000; Holdsworth et al., 2006). The pressure, P , was obtained from NRLMSISE-00 for
 187 consistency with the turbulence calculations. In the derivations by Dyrland et al. (2010) and
 188 Hall et al. (2012), for example, temperatures were then normalized to independent
 189 measurements by the MLS (Microwave Limb Sounder) on board the EOS (Earth Observing
 190 System) Aura spacecraft launched in 2004. The MLS measurements were chosen because the
 191 diurnal coverage was constant for all measurements and it was therefore simpler to estimate
 192 values that were representative of daily means, than other sources such as SABER. In this
 193 way, the influence of any systematic deficiencies in NRLMSISE-00 (e.g. due to the age of the
 194 model) were minimized.

195

196 **Results and implications for changing neutral air temperature**

197 Following the method described above and by Hall et al. (1998b and 2008), the turbopause
 198 position is determined as shown in Fig. 1. The time and height resolutions of the MF radars
 199 used for the investigation are 5 minutes and 3 km respectively, and daily means of turbulent
 200 energy dissipation rate profiles are used to determine corresponding turbopause altitudes. The
 201 Figure shows the evolution since 1999, 70°N, 19°E (Tromsø) in the upper panel and 52°N,
 202 107°W (Saskatoon) in the lower panel. Results are, of course specific to these geographical
 203 locations and it must be stressed that they are in no way zonally representative (hereafter,
 204 though, "70°N" and "52°N" may be used to refer to the two locations for convenience). Data
 205 are available from 1 January 1999 to 25 June 2014 for Saskatoon but thereafter, technical
 206 problems affected data quality. Data are shown from 1 January 1999 to 25 October 2015 for

207 Tromsø. The cyan background corresponding to the period 16 February 1999 to 16 October
208 2000 in the 70°N (Tromsø) panel indicates data available but using different experiment
209 parameters and thus 70°N data prior to 17 October 2000 are excluded from this analysis. A
210 30-day running mean is shown by the thick lines with the shading either side indicating the
211 standard deviation. The seasonal variation is clear to see, and for illustrative purposes, trend
212 lines have been fitted to June and December values together with hyperbolae showing the
213 95% confidence limits in the linear fits (Working and Hotelling, 1929); the seasonal
214 dependence of the trends is addressed in more detail subsequently. The months of June and
215 December are chosen simply because these correspond to the solstices and thus to avoid any
216 a priori conception of when one could anticipate the maxima and minima to be. It is evident
217 that, apart from the seasonal variation, the mid-latitude turbopause changes little over the
218 period 1999-2014, whereas at high latitude there is more change for the summer state over
219 the period 2001-2015 (the summers of 1999 and 2000 being excluded from the fitting due to
220 changes in experiment parameters for the Tromsø radar). To investigate the seasonal
221 dependence of the change further, the monthly values for 70°N and 52°N are shown in Fig. 2.
222 Since 2001, the high latitude turbopause has increased in height during late spring and mid-
223 summer but otherwise remained constant. Since individual months are selected the possibility
224 of "end-point" biases are not an issue in the trend-line fitting as would be the case if
225 analyzing entire datasets with non-integer numbers of years. Even so, certain years may be
226 apparently anomalous, for example the summer of 2003. In this study, the philosophy is to
227 look for any significant change in the atmosphere over the observational period. If anomalous
228 years are caused by, for example, changes in gravity-wave production (perhaps due to an
229 increasing frequency of storm in the troposphere) and filtering in the underlying atmosphere,
230 these too should be considered part of climate change. The trend (or overall change) over the
231 observation period is indeed sensitive to exclusion of certain years. Although not illustrated

232 here, this was tested briefly: selecting data from only 2004 onwards indicates no significant
233 change for summer, but a slightly increased negative winter change (to $-1.7 \pm 0.2 \text{ K decade}^{-1}$);
234 excluding only 2003 (the visually anomalous year) fails to alter the summer and winter values
235 significantly at all. The above findings represent an update of those by Hall et al. (1998b and
236 2008), adding more years to the time series and therefore now covering a little over one solar
237 cycle (the latter half of cycle 23 and first half of 24). As for the preceding papers and for
238 consistency the neutral atmosphere parameters (temperature and density) required have been
239 obtained from the NRLMSISE-00 empirical model (Picone et al., 2002) and have been
240 assumed not to exhibit any trend over the observation period. In other terms, one-year
241 seasonal climatology temperature models at one-day resolution for 70°N and 52°N and
242 altitude range appropriate for the respective radars are therefore used for all years for
243 consistency with earlier results and for consistency between the two latitudes studied here.
244 Satellite-based temperature determinations are, of course available, including, for example
245 SABER (Sounding of the Atmosphere by Broadband Emission Radiometry) on board
246 TIMED (Thermosphere Ionosphere Mesosphere Energetics and Dynamics) which was
247 launched in 2001. The temporal sampling by such instruments makes the estimation of (for
248 example) daily means somewhat complicated. Moreover, the measurements are not
249 necessarily representative for the field of field of view of the radar because the geographical
250 coverage of remote sensing data needs to be sufficiently large to obtain the required annual
251 coverage, since the sampling region can vary with season (depending on the satellite). Choice
252 of the somewhat dated NRLMSISE-00 model at least allows the geographical location to be
253 specified and furthermore ensures a degree of consistency between the two sets of radar
254 observations and also earlier analyses. The only ground-based temperature observations both
255 available and suitable are at 70°N and 90 km altitude as described earlier and used
256 subsequently.

257 Next, we have attempted to investigate the effects of changing temperature. In a very
258 simplistic approach, hypothetical altitude-invariant trends are imposed on the NRLMSISE-00
259 profiles. In other words, the same hypothetical trend is applied to all heights (for want of
260 better information) in the NRLMSISE-00 profile to generate evolving (cooling or warming)
261 temperature time-series. The suggested trends vary from -20Kdecade^{-1} to $+20\text{Kdecade}^{-1}$, thus
262 well encompassing any realistically conceivable temperature change (c.f. Blum and Fricke,
263 2008; Danilov, 1997, Lübken, 1999). The result of applying hypothetical temperature trends
264 to the time-invariant turbopause heights shown earlier is demonstrated in Figure 3. Given the
265 seasonal differences identified earlier, four combinations are shown: summer (average of
266 May, June and July) and winter (average of November, December and January) for each
267 geographic location. Realistic temperature trends can be considered within the range ± 6
268 Kdecade^{-1} such that the only significant response of turbopause height to temperature trend is
269 for 70°N in summer. In addition, the figure includes estimated trends obtained from
270 observations, which shall be explained forthwith. The salient point arising from the Figure is
271 that no realistic temperature trend (at least given the simple model employed here) has the
272 capability of reversing the corresponding trend in turbopause height.

273 In a recent study, Holmen et al. (2015) have built on the method of Hall et al. (2012) to
274 determine 90 km temperatures over NTMR, as has been described in the previous section.
275 This new work presents more sophisticated approaches for normalisation to independent
276 measurements and investigating the dependence of derived temperatures on solar flux.
277 Having removed seasonal and solar cycle variations in order to facilitate trend-line fitting (as
278 opposed to isolating a hypothetical anthropogenic-driven variation), Holmen et al. (2015)
279 arrive at a temperature trend of $-3.6 \pm 1.1 \text{Kdecade}^{-1}$ determined over the time interval 2004-
280 2014 inclusive. This can be considered statistically significant (viz. significantly non-zero at

281 the 5% level) since the uncertainty ($2\sigma = 2.2 \text{ Kdecade}^{-1}$) is less than the trend itself (e.g. Tiau
282 et al., 1990).

283 Estimation of changes in temperature corresponding to the period for determination of the
284 turbopause were only viable for 70°N , these being $-0.8 \pm 2.9 \text{ Kdecade}^{-1}$ for summer and -8.1
285 $\pm 2.5 \text{ Kdecade}^{-1}$ for winter, and these results are indicated in Fig. 3. Again using the simple
286 idea of superimposing a gradual temperature change (the same for all heights) on the
287 temperature model used for the turbulence determination thus fails to alter the change in
288 turbopause height significantly, for the \sim decade of observations. Although direct temperature
289 measurements are not available for the 52°N site, Offermann et al, (2010) report cooling rates
290 of $\sim 2.3 \text{ K decade}^{-1}$ for 51°N , 7°E , and She et al. (2015) $\sim 2.8 \text{ K decade}^{-1}$ for 42°N , 112°W . As
291 for 70°N , these results do not alter the conclusions inferred from Fig. 3.

292

293 **Discussion**

294 The aim of this study has been to update earlier reports (viz. Hall et al. 2008) of turbopause
295 altitude and change determined for two geographic locations: 70°N , 19°E (Tromsø) and
296 52°N , 107°W (Saskatoon). An effort has been made to demonstrate that conceivable
297 temperature trends are unable to alter the overall results, viz. that there is evidence of
298 increasing turbopause altitude at 70°N , 19°E in summer, but otherwise no significant change
299 during the period 2001 to 2014. Assimilating results from in situ experiments spanning the
300 time interval 1966-1992, Pokhunkov et al. (2009) present estimates of turbopause height
301 trends for several geographical locations, but during a period prior to that of our observations.
302 For high latitude the turbopause is reported to have fallen by $\sim 2\text{-}4 \text{ km}$ between 1968 and
303 1989 – the opposite sign of our finding for 2001-2014. More recently, further evidence has
304 been presented for a long-term descent of the turbopause, at least at mid-latitude (Oliver et
305 al., 2014 and references therein). The rationale for this is that the atomic oxygen density [O]

306 has been observed to increase during the time interval 1975-2014 at a rate of approximately
 307 1% year⁻¹. The associated change in turbopause height may be estimated thus:

$$308 \quad H = RT / mg \quad (10)$$

309 where H is scale height, R is the universal gas constant ($=8.314 \text{ J mol}^{-1} \text{ K}^{-1}$), m is the mean
 310 molecular mass (kg mol^{-1}) and g is the acceleration due to gravity. At 120 km altitude, g is
 311 taken to be 9.5 ms^{-2} . For air and atomic oxygen, $m = 29$ and 16 respectively. For a typical
 312 temperature of 200K, the two corresponding scale heights are therefore $H_{air} = 6.04 \text{ km}$ and
 313 $H_{oxygen} = 10.94 \text{ km}$. If the change (fall) in turbopause height is denoted by Δh_{turb} , then Oliver
 314 et al. (2014) indicate that the factor by which [O] would increase is given by:

$$315 \quad \exp(\Delta h_{turb} / H_{air}) / \exp(\Delta h_{turb} / H_{oxygen}) \quad (11)$$

316 Note that Oliver et al. (2014) state that '[O] ... would increase by the amount', but, since Eq.
 317 (11) is dimensionless, the reader should be aware this is a factor, not an absolute quantity. At
 318 first, there would appear to be a fundamental difference between the findings derived from
 319 [O] at a mid-latitude station and those for ϵ from a high-latitude station, and indeed the
 320 paradox could be explained by either the respective methods and/or geographic locations.
 321 Usefully, in this context, Shinbori et al. (2014) and Kozubek et al. (2015) investigate such
 322 geographical diversity. However if one examines the period from 2002 onwards
 323 (corresponding to the high-latitude dataset, but only about one quarter of that from the mid-
 324 latitude station), a decrease in [O] corresponds with an increase in Δh_{turb} . If, then, Δh_{turb} for
 325 the measured summer temperature change at high latitude (viz. $0.16 \text{ km year}^{-1}$ from Fig. 3) is
 326 inserted in Eq. (11) together with the suggested scale heights for air and atomic oxygen, one
 327 obtains a corresponding decrease in [O] of $16\% \text{ decade}^{-1}$, e.g. over the period 2002-2015. The
 328 corresponding time interval is not analysed per se by Oliver et al (2014) but a visual
 329 inspection suggests a decrease of the order of 20%; the decrease itself is incontrovertible and
 330 therefore in qualitative agreement with our high-latitude result.

331 It is somewhat unfortunate that it is difficult to locate simultaneous and approximately co-
332 located measurements by different methods. The turbopause height-change derived by Oliver
333 et al. (2014) are by measurements of [O] and at mid-latitude; those by Pokhunkov et al.
334 (2009), also by examining constituent scale-heights, include determinations for Heiss Island
335 (80°N, 58°E) but this rocket sounding programme was terminated prior to the start of our
336 observation series (Danilov et al., 1979). It should be noted, however that the results of
337 seasonal variability presented by Danilov et al. (1979) agree well with those described here
338 giving credence to the method and to the validity of the comparisons above.

339 Finally, the change in turbopause altitude during the last decade or more should be placed in
340 the context of other observations. The terrestrial climate is primarily driven by solar forcing,
341 but several solar cycles of data would be required to evaluate the effects of long-term change
342 in space weather conditions on turbulence in the upper atmosphere. A number of case-studies
343 have been reported, however that indicate how space weather events affect the middle
344 atmosphere (Jackman et al., 2005; Krivolutsky et al., 2006). One recurring mechanism is
345 forced change in stratospheric chemistry (in particular, destruction and production of ozone
346 and hydroxyl); the associated perturbations in temperature structure adjust the static stability
347 of the atmosphere through which gravity waves propagate before reaching the mesosphere. In
348 addition, greenhouse gases causing global warming in the troposphere act as refrigerants in
349 the middle atmosphere and so changing the static stability and therefore the degree to which
350 gravity waves shed turbulence en route to the UMLT. Not a subject of this study, it is
351 hypothesised that changes in the troposphere and oceans give rise to a higher frequency of
352 violent weather; this in turn could be expected to increase the overall gravity wave activity
353 originating in the lower atmosphere but propagating through the middle atmosphere. Sudden
354 stratospheric warmings (SSWs) also affect (by definition) the vertical temperature structure
355 and thus gravity wave propagation (e.g. de Wit et al., 2015; Cullens et al., 2015). Apart from

356 direct enhancements of stratospheric temperatures, SSWs have been demonstrated to affect
357 planetary wave activity even extending into the opposite hemisphere (e.g. Stray et al., 2015).
358 If such effects were capable of, for example, triggering the springtime breakdown of the polar
359 vortex, associated horizontal transport of stratospheric ozone contributes to determination of
360 the tropopause altitude (e.g. Hall, 2013) and again, gravity wave propagation. Overall change
361 in the stratosphere is proposed as the origin of the observed strengthening of the Brewer
362 Dobson circulation during the last 35 years at least (Fu et al., 2015). Closer to the 70°N, 19°E
363 (Tromsø) observations, Hoffmann et al. (2011) report increases in gravity wave activity at
364 55°N, 13°E during summer, including at 88km. Although not co-located, the increasing
365 gravity wave flux, with waves breaking at the summer high latitude mesopause would
366 similarly increase turbulence intensity and support the change reported here. Further
367 references to long-term change in the middle and upper atmosphere in general can be found
368 in Cnossen et al. (2015). Background winds and superimposed tides thus affecting gravity
369 wave propagation and filtering in the atmosphere underlying the UMLT also vary from
370 location to location at high latitude and the two studies by Manson et al. (2011a and 2011b)
371 study this zonal difference and compare with a current model. Although for approximately
372 10° further north than the Tromsø radar site, these studies give valuable background
373 information, on not only the wind field, but also on tidal amplitude perturbation due to
374 deposition of gravity waves' horizontal momentum.

375

376 **Conclusion**

377 Updated temporal evolutions of the turbopause altitude have been presented for two
378 locations: 70°N, 19°E (Tromsø) and 52°N, 107°W (Saskatoon), the time interval now
379 spanning 1999 to 2015. These turbopause altitude estimates are derived from estimates of
380 turbulent energy dissipation rate obtained from medium-frequency radars. The method entails

381 a knowledge of neutral temperature that had earlier (Hall et al., 2008) been assumed to be
382 constant with time. Here the response of the change in turbopause heights over the period of
383 the study to temperature trends - both hypothetical and observed - is examined. No
384 temperature trend scenario was capable of altering the observed turbopause characteristics
385 significantly; at 70°N, 19°E an increase in turbopause height is evident during the 1999-2015
386 period for summer months, whereas for winter at 70°N, 19°E and all seasons at 52°N, 107°W
387 the turbopause height has not changed significantly. In evaluating these results, however,
388 there are a number of caveats that must be remembered. Firstly, the radar system does not
389 perform well with an aurorally disturbed D-region - the study, on the other hand incorporates
390 well over 100,000 hours of data for each radar site, and auroral conditions are occasional and
391 of the order of a few hours each week at most. Secondly, an influence of the semi-empirical
392 model used to provide both density and Brunt-Väisälä frequencies cannot be disregarded. It
393 should also be stressed that a change is being reported for the observational periods of
394 approximately 15 years (i.e. just over one solar cycle) and parameterized by fitting linear
395 trend-lines to the data; this is distinct from asserting long-term trends in which solar and
396 anthropogenic effects can be discriminated.

397 At first, this conclusion would appear to contradict the recent report by Oliver et al. (2014)
398 and Pokhunkov et al. (2009), however, closer inspection shows that if one considers the time
399 interval 2002-2012 in isolation, there is a qualitative agreement. In fact, we note that Oliver et
400 al. (2014) deduce a turbopause change based on changing atomic oxygen concentration and
401 so we are similarly able to deduce a change in atomic oxygen concentration based on the
402 change in turbopause height obtained from direct estimation of turbulence intensity. Given an
403 average (i.e. not differentiating between seasons) temperature change of $-3.4 \pm 0.5 \text{ K decade}^{-1}$
404 for 70°N, 19°E (Tromsø), the change in turbopause height in summer over the same time
405 interval is $1.6 \pm 0.3 \text{ km decade}^{-1}$ suggesting a decrease in atomic oxygen concentration of 16%.

406 The primary result of this study is to demonstrate the increasing altitude of the summer
407 turbopause at 70°N, 19°E and the apparently unvarying altitude in winter and at 52°N,
408 107°W during the time interval 1999-2014. Independent studies using a radically different
409 method demonstrate how to infer a corresponding decrease in atomic oxygen concentration,
410 as a spin-off result. Finally, the question as to the exact mechanism causing the evolution of
411 turbulence in the lower thermosphere at, in particular 70°N, 19°E, remains unanswered, and
412 furthermore, dynamics at this particular geographic location may be pathological. The
413 solution perhaps lies in seasonally dependent gravity wave filtering in the underlying
414 atmosphere being affected by climatic tropospheric warming and/or middle atmosphere
415 cooling; hitherto, however, this remains a hypothesis.

416

417 **Acknowledgements**

418 The authors thank the referees of this paper.

419

420

421

422 Table 1. Salient radar parameters

Parameter	Tromsø	Saskatoon
Geographic coordinates	69.58°N, 19.22°E	52.21°N, 107.11°E
Operating frequency	2.78 MHz	2.22 MHz
Pulse length	20 μ s	20 μ s
Pulse repetition frequency	100 Hz	60 Hz
Power (peak)	50 kW	25 kW
Antenna beamwidth	17° at -3dB	17° at -6dB
Altitude resolution	3 km	3 km
Time resolution (post-analysis)	5 min	5 min

423

424

425

426 **References**427 Batchelor, G. K.: *The theory of homogeneous turbulence*, 197pp, Athenaceum Press Ltd.,

428 Newcastle-upon-Tyne, Great Britain, 1953.

429 Blum, U. and Fricke, K. H.: Indications for a long-term temperature change in the polar

430 summer middle atmosphere, *J. Atmos. Solar-Terr. Phys.*, 70, 123-137, 2008

431 Briggs, B. H.: Radar observations of atmospheric winds and turbulence: a comparison of

432 techniques, *J. Atmos. Terr. Phys.*, 42, 823-833, 1980.

433 Cervera, M.A. and Reid, I. M.: Comparison of atmospheric parameters derived from meteor

434 observations with CIRA, *Radio Sci.*, 35, 833-843, 2000.

435 Cullens, C. Y., England, S. L. and Immel, T. J.: Global responses of gravity waves to

436 planetary waves during stratospheric sudden warming observed by SABER, *J. Geophys.*437 *Res.*, 120, doi:10.1002/2015JD023966, 2015.

438 Chilson, P.B., Czechowsky, P. and Schmidt, G.: A comparison of ambipolar diffusion

439 coefficients in meteor trains using VHF radar and UV lidar, *Geophys. Res. Lett.*, 23,

440 2745-2748, 1996.

441 Cnossen, I., Laštovička, J. and Emmert, J. T.: Introduction to special issue on "Long-term

442 changes and trends in the stratosphere, mesosphere, thermosphere and ionosphere", *J.*443 *Geophys. Res.*, 120, doi:10.1002/2015JD024133, 2015.

444 Danilov, A. D., Kalgin, U. A. and Pokhunov, A. A.: Variation of the mesopause level in polar

445 regions, *Space Res. XIX*, 83, 173-176, 1979.

- 446 Dyrland, M. E., Hall, C. M., Mulligan, F. J., and Tsutsumi, M.: Improved estimates for
447 neutral air temperatures at 90 km and 78°N using satellite and meteor radar data, *Radio*
448 *Science*, *45*, RS4006, doi: 10.1029/2009RS004344, 2010.
- 449 Fu, Q., Lin, P., Solomon, S. and Hartmann, D. L.: Observational evidence of the
450 strengthening of the Brewer-Dobson circulation since 1980, *J. Geophys. Res.*, *120*, doi:
451 10.1002/2015JD023657, 2015.
- 452 Fukao, S., Yamanaka, M. D., Ao, N., Hocking, W. K., Sato, T., Yamamoto, M., Nakamura,
453 T., Tsuda, T. and Kato, S.: Seasonal variability of vertical eddy diffusivity in the middle
454 atmosphere, 1. Three-year observations by the middle and upper atmosphere radar, *J.*
455 *Geophys. Res.*, *99*, 18,973-18,987, 1994.
- 456 Hall, C. M.: The Ramfjormoen MF radar (69°N, 19°E): Application development 1990-2000,
457 *J. Atmos. Solar-Terr. Phys.*, *63*, 171-179, 2001.
- 458 Hall, C.M.: The radar tropopause above Svalbard 2008-2012: characteristics at various
459 timescales, *J. Geophys. Res.*, *118*, doi:10.1002/jgrd50247, 2013.
- 460 Hall, C.M., Blix, T. A., Thrane, E. V., and F.-J. Lübken: Seasonal variation of mesospheric
461 turbulent kinetic energy dissipation rates at 69°N, *proc. 13th ESA symposium.*, 505-509,
462 1997.
- 463 Hall, C. M., Manson, A. H. and Meek, C. E.: Measurements of the arctic turbopause, *Ann.*
464 *Geophys.*, *16*, 342-345, 1998a.
- 465 Hall, C. M., Manson, A. H. and Meek, C. E.: Seasonal variation of the turbopause: One year
466 of turbulence investigation at 69° N by the joint University of Tromsø / University of
467 Saskatchewan MF radar, *J. Geophys. Res.*, *103*, 28769-28773, 1998b.
- 468 Hall, C.M., Aso, T., Tsutsumi, M., Nozawa, S., Manson, A. H. and Meek, C. E.: Testing the
469 hypothesis of the influence of neutral turbulence on deduction of ambipolar diffusivities
470 from meteor trail expansion, *Annales Geophys.*, *23*, 1071-1073, 2005.

- 471 Hall, C. M, Brekke, A., Manson, A. H., Meek, C. E., and Nozawa, S.: Trends in mesospheric
472 turbulence at 70°N, *Atmos. Sci. Lett.*, 8, 80-84, doi:10.1002/asl.156 2007a.
- 473 Hall, C.M., Meek, C. E., Manson, A. H., and Nozawa, S.: Turbopause determination,
474 climatology and climatic trends, using medium frequency radars at 52° and 70°N, *J.*
475 *Geophys. Res.*, 113, D13104, doi:10.1029/2008JD009938, 2008.
- 476 Hall, C.M., Dyrland, M. E., Tsutsumi, M., and Mulligan, F.: Temperature trends at 90km
477 over Svalbard seen in one decade of meteor radar observations, *J. Geophys. Res.* 117,
478 D08104, doi:10.1029JD017028, 2012.
- 479 Hocking, W. K.: On the extraction of atmospheric turbulence parameters from radar
480 backscatter Doppler spectra – I. Theory, *J. Atmos. Terr. Phys.*, 45, 89-102, 1983.
- 481 Hocking, W. K.: An assessment of the capabilities and limitations of radars in measurements
482 of upper atmosphere turbulence, *Adv. Space Res.*, 17, (11)37-(11)47, 1996.
- 483 Hoffmann, P., Rapp, M., Singer, W. and Keuer, D.: Trends of mesospheric gravity waves at
484 northern middle latitudes during summer, *J. Geophys. Res.*, 116,
485 doi:10.1029/2011JD015717, 2011.
- 486 Holdsworth, D.A., Morris, R. J., Murphy, D. J., Reid, I. M., Burns, G. B. and French, W. J.
487 R.: Antarctic mesospheric temperature estimation using the Davis MST radar, *J.*
488 *Geophys. Res.*, 111, D05108, doi:10.1029/2005JD006589, 2006.
- 489 Holmen, S. E., Hall, C. M. and Tsutsumi, M.: Neutral atmosphere temperature change at
490 90km, 70°N, 19°E, 2003-2014, *Atmos. Chem. Phys. Discuss.*, 15, 15319-15354,
491 doi:10.5194/acpd-15-15319-2015, 2015.
- 492 Jackman, C. H., DeLand, M. T., Labow, G. J., Fleming, E. L., Weisenstein, D. K., Ko, M. K.
493 W., Sinnhuber, M., Anderson, J. and Russel, J. M.: The influence of the several very large

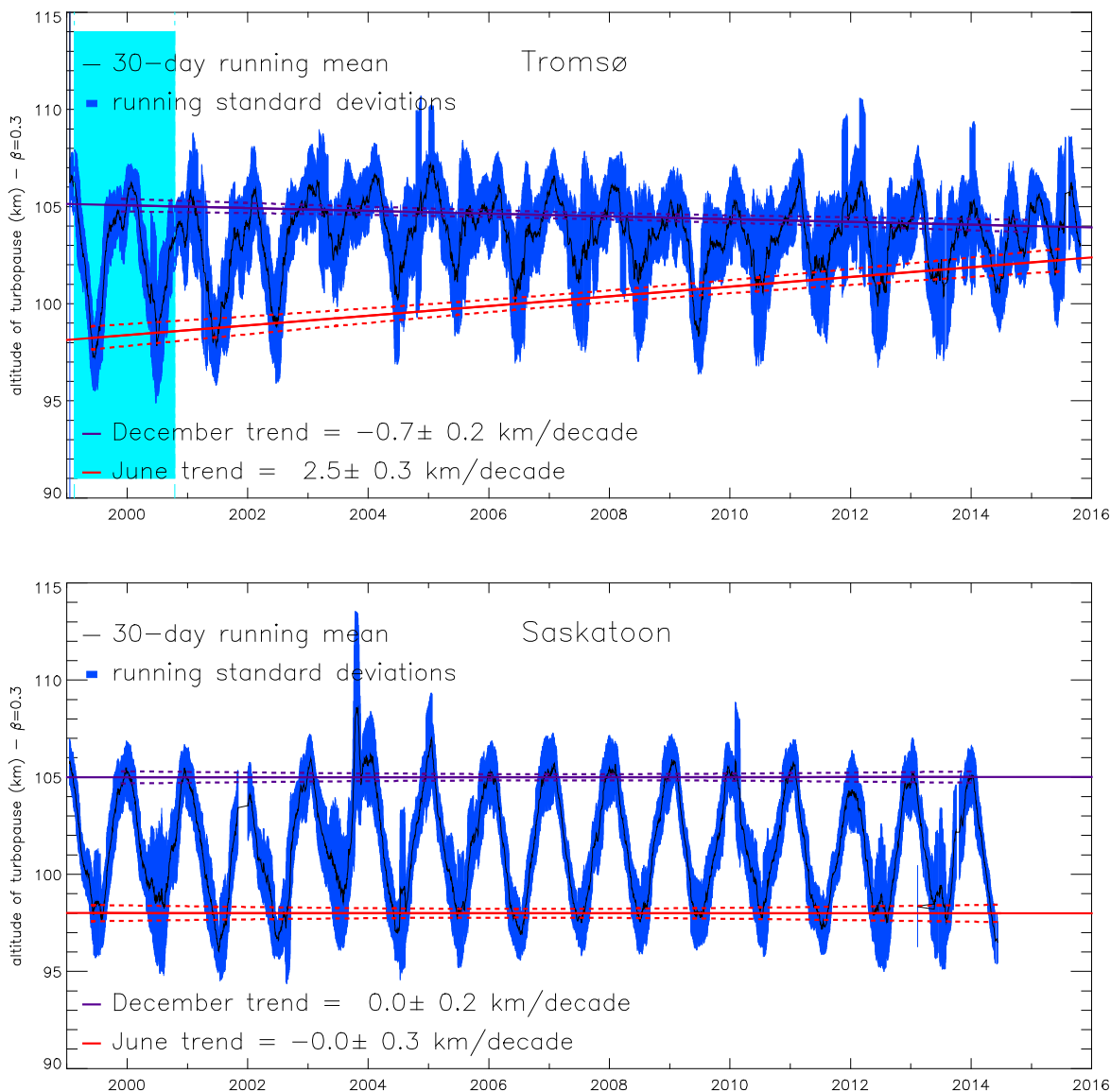
- 494 solar proton events in years 2000-2003 on the middle atmosphere, *Adv. Space Res.*, 35,
495 445-450, doi:10.1016/j.asr.2004.09.006, 2005.
- 496 Kozubek, M., Križan, P. and Laštovička, J.; Northern Hemisphere stratospheric winds in
497 higher midlatitudes: longitudinal distribution and long-term trends, *Atmos. Chem. Phys.*,
498 15, 2203-2213, doi:10.5194/acp-15-2203-2015, 2015.
- 499 Krivolutsky, A. A., Klyuchnikova, A. V., Zakharov, G. R., Vyushkova, Y. T. and Kuminov,
500 A. A.: Dynamical response of the middle atmosphere to solar proton event of July 2000:
501 three dimensional model simulations, *Adv. Space Res.*, 37, 1602-1613,
502 doi:10.1016/j.asr.2005.05.115, 2006.
- 503 Kundu, P. K.: *Fluid Mechanics*, 638pp, Academic Press, San Diego, USA, 1990.
- 504 Kolmogorov, A. N.: Dissipation of energy in the locally isotropic turbulence, *Proc. USSR*
505 *Academy of Sciences*, 30, 299-303, 1941.
- 506 Lübken, F.-J.: Nearly zero temperature trend in the polar summer mesosphere, *Geophys. Res.*
507 *Lett.*, 104, 9135-9149, 1999.
- 508 Manson, A. H. and Meek, C. E.: Climatologies of mean winds and tides observed by medium
509 frequency radars at Tromsø (70°N) and Saskatchewan (52°N) during 1987-1989, *Can. J.*
510 *Phys.* 69, 966-975, 1991.
- 511 Manson, A. H., Meek, C. E., Xu, X., Aso, T., Drummond, J. R., Hall, C. M., Hocking, W. K.,
512 Tsutsumi, M. and Ward, W. E.: Characteristics of Arctic winds at CANDAC-PEARL
513 (80°N, 86°W) and Svalbard (78°N, 16°E) for 2006-2009: radar observations and
514 comparisons with the model CMAM-DAS, *Ann. Geophys.*, 29, 1927-1938,
515 doi:10.5194/anngo-29-1927-2011, 2011a.
- 516 Manson, A. H., Meek, C. E., Xu, X., Aso, T., Drummond, J. R., Hall, C. M., Hocking, W. K.,
517 Tsutsumi, M. and Ward, W. E.: Characteristics of Arctic tides at CANDAC-PEARL
518 (80°N, 86°W) and Svalbard (78°N, 16°E) for 2006-2009: radar observations and

- 519 comparisons with the model CMAM-DAS, *Ann. Geophys.*, 29, 1927-1938,
520 doi:10.5194/anngeo-29-1927-2011, 2011b.
- 521 McIntyre, M. E.: On dynamics and transport near the polar mesopause in summer, *J.*
522 *Geophys. Res.*, 94, 20841-20857, 1991.
- 523 McKinley, D. W. R.: *Meteor Science and Engineering*, 309 pp, McGrath-Hill, New York,
524 1961.
- 525 Oakey, N. S.: Determination of the rate of dissipation of turbulent energy from simultaneous
526 temperature and velocity shear microstructure measurements, *J. Phys. Oceanogr.*, 12, 256-
527 271, 1982.
- 528 Offermann, D., Jarisch, M., Schmidt, H., Oberheide, J., Grossmann, K. U., Gusev, O., Russell
529 III, J. M., and Mlynczak, M. G.: The "wave turbopause", *J. Atmos. Solar-Terr. Phys.*, 69,
530 2139-2158, 2007.
- 531 Offermann, D., Hoffmann, P., Knieling, P., Koppmann, R., Oberheide, J., and Steinbrecht,
532 W.: Long-term trends and solar cycle variations of mesospheric temperature and
533 dynamics, *J. Geophys. Res.*, 115, 2156-2202, D18127, doi:10.1029/2009JD013363, 2010.
- 534 Oliver, W. L., Holt, J. M., Zhang, S.-R., and Goncharenko, L. P.: Long-term trends in
535 thermospheric neutral temperature and density above Millstone Hill, *J. Geophys. Res.*,
536 *Space Phys.* 119, 1-7, doi:10.1002/2014JA020311, 2014.
- 537 Pardjac, E. R., Monti, P. and Fernando, H. J. S.: Flux Richardson number measurements in
538 stable atmospheric shear flows, *J. Fluid Mech.*, 459, 307-316,
539 doi:10.1017/S0022112002008406, 2002.
- 540 Picone, J. M., Hedin, A. E., Drob, D. P., Atkin, A. C.: NRLMSISE-00 empirical model of the
541 atmosphere: statistical comparisons and scientific issues, *J. Geophys. Res.*, 107 (A12),
542 1468, doi:10.1029/2002JA009430, 2002.

- 543 Pokhunkov, A. A., Rybin, V. V. and Tulinov, G. F.: Quantitative characteristics of long-term
544 changes in parameter of the upper atmosphere of the Earth over the 1966-1992 period,
545 *Cosmic Res.* 47, 480-490, 2009
- 546 Schlegel, K., Brekke, A. and Haug, A.: Some characteristics of the quiet polar D-region and
547 mesosphere obtained with the partial reflection method, *J. Atmos. Terr. Phys.*, 40, 205-
548 213, 1978.
- 549 She, C.-Y-, Krueger, D. A. and Yuan, T.: Long-term midlatitude mesopause region
550 temperature trend deduced from quarter century (1990-2014) Na lidar observations, *Ann.*
551 *Geo. Comm.* 33, 363-369, doi:10.5194/angeocom-33-363-2015, 2015.
- 552 Shinbori, A., Koyama, Y., Nose, M., Hori, T., Otsuka, Y. and Yatagai, A.: Long-term
553 variation in the upper atmosphere as seen in the geomagnetic solar quiet daily variation,
554 *Earth, Planets and Space*, 66, 155-175, doi: 10.1186/s40623-014-0155-1, 2014.
- 555 Stray, N. H., Orsolini, Y. J., Espy, P. J., Limpasuvan, V. and Hibbins, R. E.: Observations of
556 planetary waves in the mesosphere-lower thermosphere during stratospheric warming
557 events, *Atmos. Chem. Phys.*, 15, 4997-5005, doi:10.5194/acp-15-4997-2015, 2015.
- 558 Tiao, G. C., Reinsel, G. C., Xu, D., Pedrick, J. H., Zhu, X., Miller, A. J., DeLuisi, J. J.,
559 Mateer, C. L. and Wuebbles, D. J.: Effects of autocorrelation and temporal sampling
560 schemes on estimates of trend and spatial correlation, *J. Geophys. Res.*, 95, D12, 20507-
561 20517, 1990.
- 562 Thrane, E.V., Blix, T. A., Hall, C., Hansen, T. L., von Zahn, U., Meyer, W., Czechowsky, P.,
563 Schmidt, G., Widdel, H.-U. and Neumann, A.: Small scale structure and turbulence in the
564 mesosphere and lower thermosphere at high latitudes in winter, *J. Atmos. terr. Phys.*, 49,
565 751-762, 1987.

- 566 Vandeppeer, B. G. W. and Hocking, W. K.: A comparison of Doppler and spaced antenna
567 radar techniques for the measurement of turbulent energy dissipation rates, *Geophys. Res.*
568 *Lett.*, 20, 17-20, 1993.
- 569 Weinstock, J.: Vertical turbulent diffusion in a stably stratified fluid, *J. Atmos. Sci.*, 35, 1022–
570 1027, 1978.
- 571 de Wit, R. J., Hibbins, R. E., Espy, P. J. and Hennum, E. A.: Coupling in the middle
572 atmosphere related to the 2013 major sudden stratospheric warming, *Ann. Geophys.*, 33,
573 309-319, doi:10.5194/anngeo-33-309-2015, 2015.
- 574 Working, H., and Hotelling, H.: Application of the theory of error to the interpretation of
575 trends. *J. American Stat. Assoc.*, 24, 73–85, 1929.
- 576

577

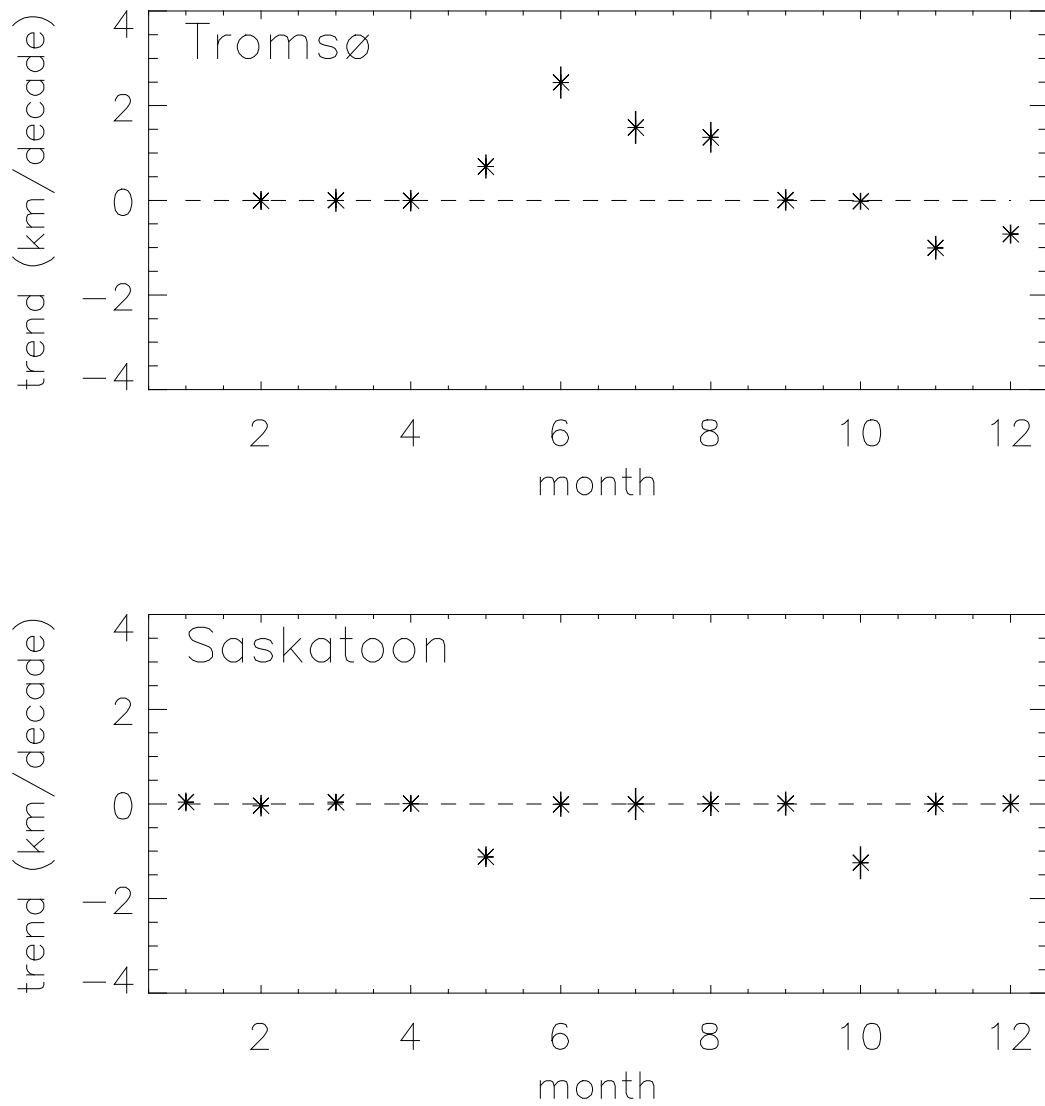


578

579 Figure 1. Turbopause altitude as determined by the definition and method described in this
 580 paper. The thick solid line shows the 30-day running mean and the shading behind it the
 581 corresponding standard deviations. The straight lines show the fits to summer and winter
 582 portions of the curve. Upper panel: 70°N (Tromsø); lower panel: 52°N (Saskatoon). The cyan
 583 background in the 70°N panel indicates data available but unused here due to different
 584 experiment parameters

585

586

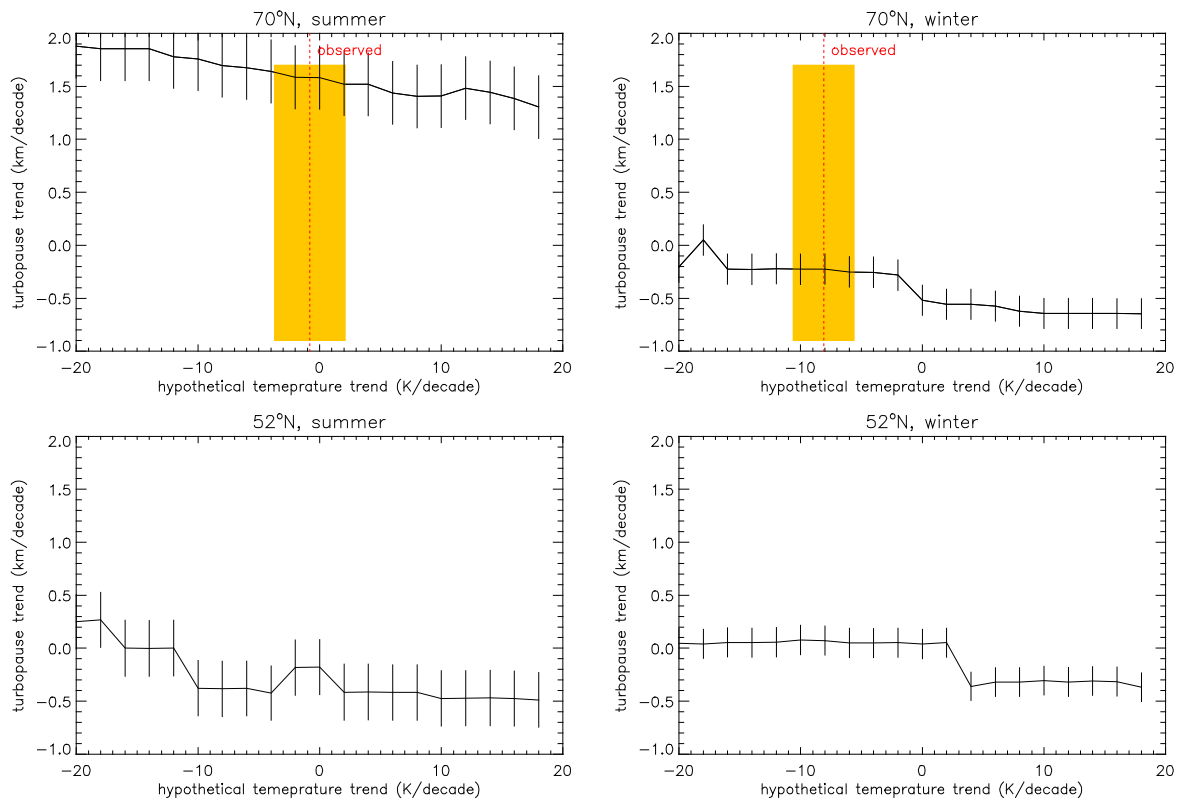


587

588 Figure 2. Trends for the period as a function of month. . Upper panel: 70°N (Tromsø); lower
589 panel: 52°N (Saskatoon).

590

591



592

593 Figure 3. Response of turbopause trend line to different upper-mesosphere/lower-
 594 thermosphere temperature trends. Hypothetical trends range from an unrealistic cooling of
 595 20K/decade to a similarly unrealistic warming. Top-left: 70°N summer (average of May, June
 596 and July); top-right: 70°N winter (average of November, December and January); bottom-
 597 left: 52°N summer; bottom-right: 52°N winter. Observed values for 70°N are also identified
 598 on the upper panels (dashed vertical lines) together with uncertainties (shading).

599